J. Biochem. 127, 199–204 (2000)

Analysis of Conformational Changes at the Unique Loop Adjacent to the ATP Binding Site of Smooth Muscle Myosin Using a Fluorescent Probe

Shinsaku Maruta,[1] Junya Saitoh, and Tsuyoshi Asakura

Department of Bioengineering, Faculty of Engineering, Soka University, Hachioji, Tokyo 192–8577

Received September 7, 1999; accepted October 28, 1999

Recent crystallographic studies have shown that smooth muscle myosin has three highly conserved unique loops, loop B (320–327), loop M (687–699), and loop N (125–134), similar to other myosins, skeletal muscle and dictyostelium myosins. We previously demonstrated that the effect of actin is mediated by a conformational change in one of the loops, loop M comprising amino acids 677 to 689 of skeletal muscle myosin [Maruta and Homma (1998) *J. Biochem.* 124, 528–533]. In the present study, in order to clarify the role of these smooth muscle myosin loops in energy transduction, we specifically labeled the loops with a fluorescent photoreactive ADP analogue, 3′-*O*-(*N*-methylanthraniloyl)-8-azido-ADP (Mant-8-N_3-ADP), and then measured the fluorescent polarization. When Mant-8-N_3-ADP was trapped by aluminium fluoride or vanadate into the ATPase site, Mant-8-N_3-ADP was covalently incorporated into loop N (125–134). In contrast, Mant-8-N_3-ADP trapped by beryllium fluoride was covalently incorporated into both loop M (687–699) and loop N (125–134) at an almost equimolar ratio. Actin binding to smooth muscle myosin S1 (SMO-S1) labeled at only loop N (125–134) increased the polarization due to the viscosity of actin. In contrast, S1 labeled at both loops N and M showed a much smaller increase in polarization. Our results indicate that the probe at loop M (687–699) of smooth muscle myosin moved to a less hindered region, suggesting that actin binding induces conformational changes at loop M (687–699) similar to those of the corresponding loop (677–689) in skeletal muscle myosin, as previously demonstrated in our laboratory.

Key words: ATP analogue, ATP binding site, fluorescent polarization, myosin, signal transduction.

Recent crystallographic studies of motor proteins have shown that the structures of the motor domains of myosin (*1–3*) and kinesin (*4*) are highly conserved, suggesting that these motor proteins may share a common mechanism for generating energy for motility from ATP hydrolysis. Nevertheless, myosin has several unique loops, loop B, loop M, and loop N, in the region of the ATP-binding cleft that are not observed in kinesin (*1–3*). Likewise, kinesin also has specific loops, named L5 and L12 (*4*). The precise function of these loops is as yet unknown, but they may determine the characteristic properties of motor proteins, e.g., mediating the interaction between ATP- and actin-binding sites or ATP- and microtubule-binding sites.

Loop M (677–689), which is part of the 20-kDa tryptic fragment of skeletal muscle myosin subfragment-1 (SKE-S1), is unique to myosin and contributes to the structure of the ATP-binding cleft; a key feature of the loop is Lys 681, which protrudes into the ATP-binding site. Composed mainly of an α-helix, the 20-kDa fragment forms the backbone of the myosin head and extends from the actin-binding site to the regulatory region, *via* the ATP binding site, and to the hinge area of the reactive cysteine region. This arrangement suggests that the 20-kDa fragment and loop M (677–689) may provide the link through which ATPase activity is modulated by actin. We have previously reported that the fluorescent labeled photoreactive ADP analogue, Mant-8-N_3-ADP, specifically crosslinks to loop M of skeletal muscle myosin by UV irradiation (*5*). Mant-8-N_3-ADP was used as probe to monitor actin-induced conformational changes in loop M (*6*). Analysis of the actin-induced changes in fluorescence polarization and quenching confirmed that actin binding induces conformational changes at loop M (677–689) resulting in the displacement of Mant-8-N_3-ADP from the ATP-binding cleft (*6*). It has been demonstrated that the effect of actin is mediated by a conformational change in loop M, comprising amino acids 677 to 689 in skeletal muscle myosin, suggesting that loop M acts as a signal transducer mediating communication between the ATP and actin-binding sites. In contrast, Luo *et al.* (*11*)

[1] To whom correspondence should be addressed. Phone: +81-426-91-9312, Fax: +81-426-91-9312, E-mail: shinsaku@t.soka.ac.jp

Abbreviations: AlF_4^-, aluminium fluoride; BeFn, fluoroberyllate; Mant-8-N_3-ADP, 3′-*O*-(*N*-methylanthraniloyl)-8-azido-ADP; Mant-SKE-S1, Mant-8-N_3-ADP covalently crosslinked to skeletal muscle S1; Mant-SMO-S1, Mant-8-N_3-ADP covalently crosslinked to smooth muscle S1; NANDP, 2-[(4-azido-2-nitrophenyl)-amino]ethyl diphosphate; S1, myosin subfragment-1; SDS-PAGE, sodium dodecyl sulfate polyacryl amide gel electrophoresis; SKE-S1, skeletal muscle myosin S1; SMO-S1, smooth muscle myosin S1; Vi, orthovanadate.

demonstrated that actin binding has minimal effects on loops N and B of smooth muscle myosin.

Recently, Dominguez *et al.* (*3*) demonstrated that smooth muscle myosin S1 (SMO-S1) also has a unique conserved loop as seen in other myosins. It is of interest that loop M through the C-terminal tryptic fragment of SMO-S1, corresponding to the 20 kDa fragment of SKE-S1, acts as a signal transducer for myosin family motor proteins. In the present study, we specifically labeled only loop N or both loops M and N in smooth muscle myosin S1 with Mant-8-N_3-ADP and measured the fluorescent polarization induced by actin to confirm the role of the loop through C-terminal tryptic fragment of the motor domain as a signal transducer.

MATERIALS AND METHODS

Chemicals—Mant-8-N_3-ATP was prepared from 8-N_3-ATP (Sigma Chemical, St. Louis, MO) as described by Maruta *et al.* (*5*). Beryllium sulfate ($BeSO_4$) and sodium fluoride (NaF) were purchased from Wako Pure Chemical (Osaka).

Proteins—Smooth muscle myosin, myosin light chain kinase, and calmodulin were prepared from turkey gizzards as described previously (*7–9*). Smooth muscle myosin S-1 was prepared by *Staphylococcus aureus* proteinase digestion as described by Ikebe and Hartshorne (*7*). Trypsin (Type VII) and *S. aureus* protease were obtained from Sigma.

Fluorescent Labeling of S1—Mant-8-N_3-ATP was hydrolyzed to Mant-8-N_3-ADP by incubation with S1. After complete hydrolysis, 1 mM $BeSO_4$ and 5 mM NaF were added to trap Mant-8-N_3-ADP at the active site. After incubation for 1 h at 25°C, the untrapped analogue and BeFn were removed by centrifugal gel filtration on a Sephadex G-50 column equilibrated in 120 mM NaCl and 50 mM Tris-HCl (pH 8.0) (*10*). The solution containing the isolated ternary complex was then placed on ice and irradiated for 3 min with 366 nm UV light (UVL-56 16W, Ultraviolet Products).

Removal of Noncovalently Bound Mant-8-N_3-ADP and BeFn—Following UV irradiation, the noncovalently bound analogue remaining in the ATPase site of SMO-S1 was removed by adding excess Mg^{2+}-ATP and actin based on the method described by Luo *et al.* (*11*). F-actin (2 ml, 100 μM) was pelleted by centrifugation at 350,000 ×*g* for 20 min at 4°C; the supernatant was discarded, and the F-actin pellet was resuspended in 2 ml of irradiated S1 solution. In the next step, 2 mM $MgCl_2$ and 2 mM ATP (pH 7.0) were added, and the solution was incubated at room temperature for 20 min to release trapped BeFn and the unincorporated Mant-8-N_3-ADP. To dissociate actin, we increased the ATP concentration to 4 mM and the ionic strength to 200 mM by the addition of KCl at 4°C. The solution was then immediately centrifuged at 350,000 ×*g* for 20 min at 4°C. EDTA (final concentration 20 mM) was added to the supernatant, which was then applied to a Sephadex G-50 centrifugal column to remove Mg^{2+}, ATP, BeFn, and the released unincorporated ATP analogue. The resulting solution containing photolabeled S1 and unmodified SMO-S1 is hereafter referred to as the purified Mant-SMO-S1. After removing the free and noncovalently bound Mant-8-N_3-ADP, the amount of fluorescent probe covalently crosslinked to the ATPase site was estimated by measuring the fluorescence intensity of the remaining photolabeled product in a solution of 5 M guanidine-HCl and 20 mM Tris-HCl (pH 7.5).

SDS-PAGE—Electrophoresis was performed in 7.5–20% polyacrylamide gradient slab gels in the presence of 0.1% SDS at a constant voltage (200 V) in the discontinuous buffer system of Laemmli (*12*).

ATPase Assay—ATPase activity was measured in the presence of 2 mM ATP at 25°C. The reaction was stopped by adding 10% trichloroacetic acid, and the released P_i was measured by the method of Youngburg and Youngburg (*13*).

Fluorescence Measurement—Fluorescence measurements were performed at 25°C with an RF-5000 Spectrofluorometer (Shimadzu). In RF-5000, monochromatic light passes through an excitation filter (360 nm) and a moving polarizer and excites fluorescent molecules in the sample. The polarized light in the sample is emitted at right angles to the incident light and passes through an emission filter (445 nm) and a vertical fixed polarizer. The emitted light is measured in both the horizontal (*Hi*) and vertical (*Iv*) planes, and polarization (*P*) is calculated from the equation $P = Iv - Hi/Iv + Hi$.

RESULTS AND DISCUSSION

Specific Labeling of Unique Loops with Mant-8-N_3-ADP—Smooth muscle myosin has three unique loops, loop B (320–327), loop N (125–134), and loop M (687–699) adjacent to the ATP binding site. These loops are structurally highly conserved as seen in skeletal muscle myosin and *Dictyostelium* myosin, as shown in Fig. 1. First, we specifically labeled loop M and loop N with fluorescent probe Mant-group *via* the formation of a transient state analogue, myosin•ADP•fluorometal ternary complexes. Previous studies have demonstrated that Mg^{2+}-ADP is trapped within the ATPase site with several types of phosphate analogues, aluminum fluoride (AlF_4^-), and beryllium fluoride (BeFn), and that vanadate causes the formation of stable myosin•ADP•phosphate analogue ternary complexes (*14–16*). We utilized the phosphate analogues to trap Mant-8-N_3-ADP within the ATP binding site of smooth muscle myosin subfragment-1 (SMO-S1) prior to UV irradiation in order to reduce nonspecific binding. The stoichiometry of the trapped Mant-8-N_3-ADP was measured as a function of Mant-8-N_3-ADP concentration (Fig. 2). Mant-8-N_3-ADP bound with high affinity in the presence of BeFn, and the bound Mant-8-N_3-ADP was saturated at approximately 0.7 mol/mol SMO-S1. Although Mant-8-N_3-ADP was also trapped in the presence of AlF_4^-, the apparent affinity was significantly lower than that seen in the presence of BeFn and saturated at 0.25 mol/mol S-1. For V_i, the bound Mant-8-N_3-ADP was saturated at 0.5 mol/mol S-1.

The ternary SMO-S1•Mant-8-N_3-ADP• AlF_4^- (BeFn or V_i) complexes were formed at a minimum concentration of Mant-8-N_3-ADP to ensure saturation with the phosphate analogues, and isolated by centrifugal gel filtration on a Sephadex G-50 column. Mant-8-N_3-ADP trapped within the active sites was covalently crosslinked into S-1 by UV irradiation. For all complexes, incorporation saturated at about 3 min as shown in Fig. 3. After photo-incorporation, the labeled S-1 (Mant-SMO-S1) was digested with trypsin, and the labeled domain was analyzed by SDS-PAGE (Fig. 4). Only the 29 kDa N-terminal fragment, which contains

loop N, was specifically labeled by AlF_4^- and V_i complexes as shown in Fig. 4 (lanes 3 and 4). Moreover, photo-affinity-labeling in the steady state (in the presence of excess Mant-8-N_3-ATP) without trapping showed a single labeling site in the 29 kDa fragment. The addition of excess ATP significantly reduced the photo-incorporation suggesting that the binding to 29 kDa is specific (Fig. 4, lanes 5 and 6). The very faint fluorescent band just under the 29 kDa fragment (lanes 3–5), which has a molecular mass slightly larger than 25 kDa may be a fragment degraded from the 29 kDa fragment. Interestingly, in the BeFn complex, the 29 kDa N-terminal and 25 kDa C-terminal fragments were labeled in almost equimolar ratios (Fig. 4, lane 2). Recent crystallographic studies of the smooth muscle myosin motor domain have shown the presence of three unique loops at the entrance of the ATPase site that have similar geometries to the loops in skeletal muscle myosin (*3*). The ADP ribose and adenine moieties in the crystal structure are very close to loop B and loop N, respectively. The amino acid side chain of Lys 691 in loop M of smooth muscle myosin also protrudes into the ATPase cleft and is close to the base part of ATP, similar to the case of Lys 681 in skeletal muscle myosin (*2*, *3*). We have previously demonstrated that for skeletal muscle myosin, Mant-8-N_3-ATP, which favors the formation of the "syn" conformation with respect to the *N*-glycoside bond of ATP, crosslinks to loop M in contrast to Mant-2-N_3-ATP, which has an "anti" conformation bound to loop N (*5*, *17*). Moreover, the 20 kDa tryptic fragment intersects the ATPase site only in the region of loop M (*6*), and, especially, only the amino acid side chain of Lys 691 in loop M is within crosslinking distance of the ATP analogues. We previously isolated the peptide (Leu 660–Lys 709) labeled by Mant-8-N_3-ADP containing loop M, which was digested completely by trypsin but showed resistance to digestion at Lys 681, which is on the middle of the peptide (*5*), suggesting that Lys 681 is modified by crosslinking with Mant-8-N_3-ADP. Therefore, it is extremely plausible that Mant-8-N_3-ADP trapped by BeFn into the active site crosslinks with loop M of SMO-S1.

We have previously suggested that the myosin•ADP•AlF_4^- and myosin•ADP•V_i ternary complexes resemble the M^{**}•ADP•P_i steady state. On the other hand, the myosin•ADP•BeFn complex shows properties intermediate between M^*•ATP and M^{**}•ADP•P_i (*14*). ^{19}F-NMR studies have clearly demonstrated that in solution BeFn incorporated into ternary complexes exists in at least four species (*18*). Moreover, the ^{19}F-NMR spectrum of an ^{19}F-labeled ADP analogue trapped into SKE-S1 with BeFn, shows two distinct adenine moiety coordinates to the site (*19*). It is proposed that the BeFn species are distinct with regard to their characteristics, and that ternary complexes containing these species may mimic different states in the ATPase cycle. Thus, one species may mimic the M^{**}•ADP•P_i state while another may mimic the M^*•ATP state. This notion appears consistent with the results that Mant-8-N_3-ADP trapped by BeFn bound to the 29 kDa and 25 kDa fragments. Species that mimic the M^{**}•ADP•P_i state may bind

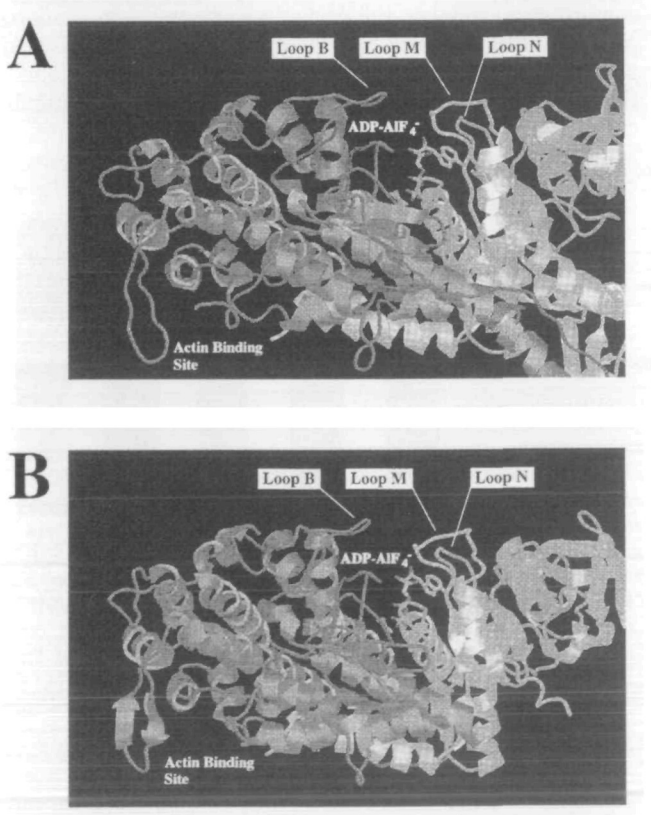

Fig. 1. **Unique, highly conserved loops surrounding the entrance to the nucleotide-binding pocket of smooth muscle myosin (A) and *Dictyostelium* myosin (B).** These photographs were prepared with the molecular graphic program Ras Mac v2.6 using the coordinate data (A: 1BR1, B: 1MND) in the protein data bank database.

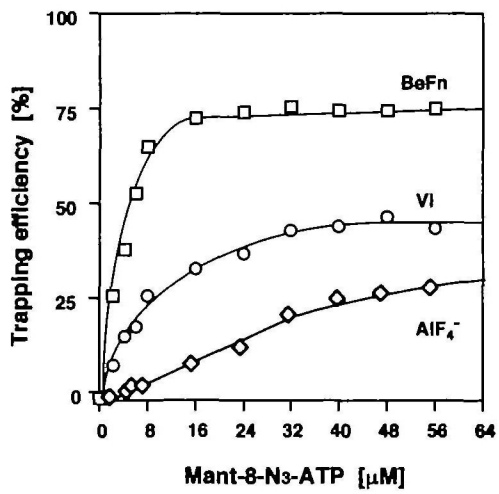

Fig. 2. **Entrapment of Mant-8-N_3-ADP within the nucleotide-binding pocket of SMO-S1 in the presence of AlF_4^-, BeFn, and vanadate.** 4 μM SMO-S1 was incubated with 2–56 μM Mant-8-N_3-ATP for 30 min in 120 mM NaCl, 30 mM Tris-HCl, pH 7.5, containing 2 mM $MgCl_2$ (for AlF_4^- and BeFn) or 1 mM $CoCl_2$ (for V_i). After Mant-8-N_3-ATP was completely hydrolyzed to Mant-8-N_3-ADP, 1 mM of AlF_4^- (◇), BeFn (□), or vanadate (○) was added to the solution, and the mixtures were incubated at 25°C for 2 h. Unbound Mant-8-N_3-ADP was removed by adding Dowex 1-x8 anion exchange resin to the solution. The amount of trapped Mant-8-N_3-ADP was estimated from the Mant-group fluorescence intensity of the analogue released from the complex by the addition of 5 M guanidine-HCl and 200 mM Tris-HCl, pH 7.5. The trapping efficiency was calculated using following equation: [trapped Mant-8-N_3-ADP (mol)/ATPase site of S-1 (mol)] × 100 (%).

to the 29 kDa fragment while other species that mimic the M**•ATP state may bind to the 25 kDa fragment. This notion may be related to the conformation of Mant-8-N_3-ADP with respect to the adenine-ribose bond. ADP analogues such as 8-N_3-ADP with bulky substitutions at the eighth position of the adenine ring favor the syn conformation in solution. The Mant-8-N_3-ADP trapped by AlF_4^- or V_i into the ATPase site may form the same anti conformation as regular ADP observed in crystal structure (*2, 3, 20*). On the contrary, the Mant-8-N_3-ADP trapped by BeFn may form either the anti or syn conformation due to the species of BeFn mentioned so far. Such a conformational difference with respect to the adenine-ribose bond may change the geometry of the adenine moiety of Mant-8-N_3-ADP in the ATPase binding site. The idea provides a possible explanation for the lower photoincorporation on AlF_4^- and V_i complexes than on the BeFn complex, because the anti conformation of 8-N_3-ADP places the 8-azido group directly over the ribose ring with which it could readily react after photolysis.

It has previously been reported that some photoreactive ADP analogues, 2-N_3-ADP and NANDP, which have an anti conformation with respect to the adenine-ribose bond or a similar conformation, photolabel Trp 130 in loop N of SKE-S1. NANDP also crosslinks to Arg 128 in scallop myosin, which is the residue equivalent to Trp 130 in SKE-S1. Therefore, it is very plausible that Mant-8-N_3-ADP crosslinks to loop N. Moreover, only the loop N region in the 29 kDa fragment faces the adenine moiety of ADP in the crystal structure (*3*).

Fluorescence Polarization of Mant-S1—The polarization of Mant-group fluorescence was measured in order to determine the effects of Mg^{2+}-ATP and actin on the mobility of Mant-8-N_3-ADP crosslinked to loop M and loop N. We prepared three S1 derivatives, which were labeled only at loop N using AlF_4^- and V_i complexes, and labeled at both loops M and N using the BeFn ternary complex as described. As shown in Fig. 5, the addition of Mg^{2+}-ATP induced a decrease in polarization, reflected by increased probe mobility for all three S-1 derivatives. We have previously observed a similar decrease in polarization for SKE-S1 labeled only at loop M as shown in Fig. 5E (*6*). The increased probe mobility is consistent with Mg^{2+}-ATP competitively displacing Mant-8-N_3-ADP from the ATP-binding site to a less hindered site outside the ATP-binding cleft. In contrast, the addition of actin to SMO-S1 derivatives induced increased polarization of the two S1 derivatives labeled only at loop N; however, SMO-S1 labeled at both loops M and N using the BeFn complex showed a much smaller increase in polarization (Fig. 5, A–D). The addition of actin to free Mant-8-N_3-ADP resulted in an increased polarization similar to that of SMO-S1s (labeled using the AlF_4^- or V_i complexes) due to the viscosity of actin. However, it has been demonstrated that SKE-S1 labeled at only loop M by Mant-8-N_3-ADP undergoes a significant decrease in polarization upon the addition of actin, suggesting that actin binding induces a conformational change at loop M to move the Mant-group to a less hindered position (*6*). The slight increase for SMO-S1 (BeFn) as shown in Fig. 5D may be due to a conformational change at loop M similar to that of loop M in SKE-S1. It can be argued that loop N is not affected by the addition of actin, but loop M changes its conformation to allow the probe to move to a less hindered position similar to SKE-S1. The present results support our previous proposal that the surface of loop M at the end of the ATPase site cleft, which is highly conserved among dif-

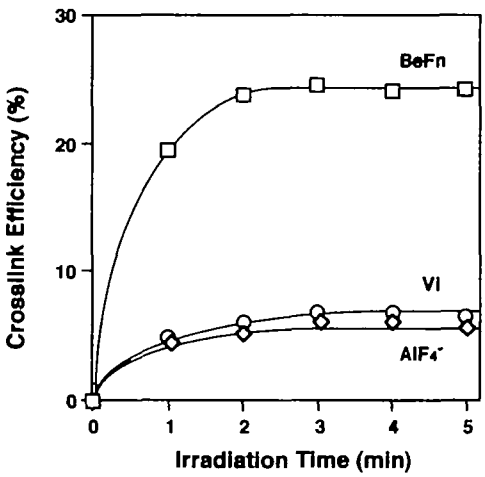

Fig. 3. **Photoincorporation of Mant-8-N_3-ADP into S-1.** Excess Mant-8-N_3-ADP was removed on a Sephadex G-50 spin column. The isolated complex was placed on ice and irradiated at 366 nm using an ultraviolet lamp (UVL-56, 16 W, Ultra Violet Products) for 1–5 min from a distance of 2 cm above the surface of the stirred solution. After irradiating for selected periods of time, the samples were precipitated by the addition of 10% trichloroacetic acid. The pellets were neutralized with 20 mM Tris-HCl, pH 7.5, and the amount of incorporated Mant-8-N_3-ADP was estimated as described above. The crosslinking efficiency was calculated from the following equation: [covalently crosslinked Mant-8-N_3-ADP (mol)/ ATPase site of S-1 (mol)] × 100 (%).

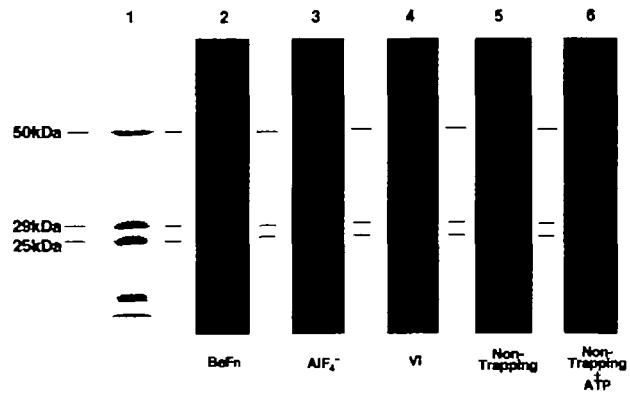

Fig. 4. **SDS-PAGE of SMO-S1 labeled with Mant-8-N_3-ADP in the presence of AlF_4^-, BeFn, or vanadate.** The ternary complexes were produced in solutions of 120 mM NaCl, 30 mM Tris-HCl, pH 7.5, and $MgCl_2$ containing 30 μM S-1 with 60 μM Mant-8-N_3-ADP + 1 mM BeFn (lane 2), 480 μM Mant-8-N_3-ADP + 1 mM AlF_4^- (lane 3) or 150 μM Mant-8-N_3-ADP + 1 mM $CoCl_2$ + 1 mM vanadate (lane 4). After incubation for 2 h, the complex was purified on a Sephadex G-50 spin column. The complex was irradiated at 366 nm for 5 min. The irradiated complexes were digested with trypsin (1/100, by mass) for 5 min at 25°C. Non-trapping photo-affinity-labeling was performed under the following conditions: 5-min irradiation at 0°C in a solution containing 30 μM S-1, 150 μM Mant-8-N_3-ATP, 120 mM NaCl, 30 mM Tris-HCl pH 7.5, and 2 mM $MgCl_2$ in the absence (lane 5) or presence of 2 mM ATP (lane 6). Lane 1 is the protein staining of trypsin digested SMO-S1.

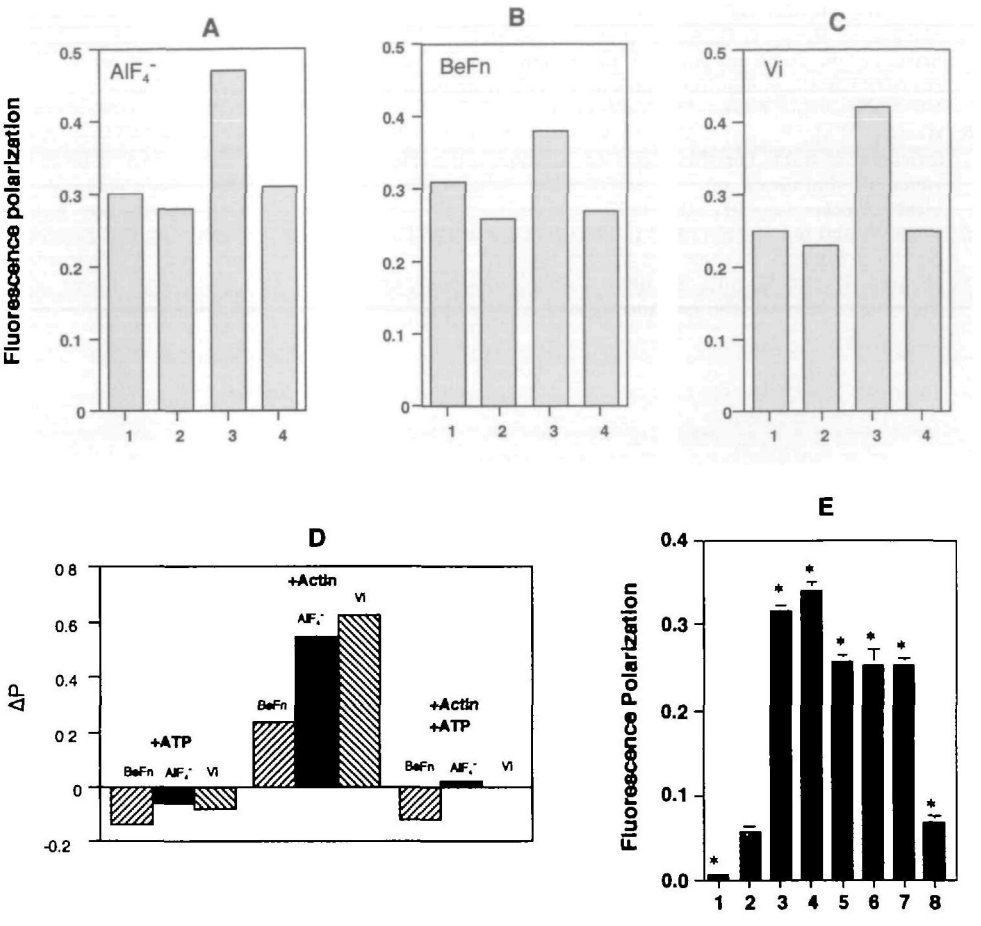

Fig. 5. **A–C: Polarization of fluorescent emissions of SMO-S1 labeled with Mant-8-N_3-ADP using AlF_4^- (A), BeFn (B), or V_i (C) in the absence and presence of ligands.** For A–C, (1) 0.5 μM Mant-SMO-S1; (2) 0.5 μM Mant-SMO-S1 + 2 mM ATP; (3) 0.5 μM Mant-SMO-S1 + 2.5 μM actin; (4) 0.5 μM Mant-SMO-S1 + 2.5 μM actin + 2 mM ATP. Samples were measured in buffer containing 120 mM NaCl, 30 mM Tris-HCl, pH 7.5, and 2 mM $MgCl_2$. **D: Relative changes in polarization (ΔP) induced by actin and ATP were calculated from the data shown in A, B, and C using the following equation: $\Delta P = (P-P_0)/P_0$, where P_0 is fluorescence polarization for Mant-S1 in the absence of ligands and P is fluorescence polarization in the presence of actin, ATP or actin + ATP. E: Polarization of the fluorescence emission of SKE-S1 labeled with Mant-8-N_3-ADP using BeFn in the absence and presence of ligands.** (1) Free Mant-8-N_3-ADP; (2) (1) + 0.25 μM actin; (3) 0.5 μM Mant-SKE-S1; (4) 0.5 μM Mant-SKE-S1 + 1 mM BeFn; (5) 0.5 μM Mant-SKE-S1 + 2 mM ATP; (6) 0.5 μM Mant-SKE-S1 + 2.5 μM actin; (7) 0.5 μM Mant-SKE-S1 + 2 mM ATP + 2.5 μM actin; (8) 0.5 μM Mant-SKE-S1 + 5 M guanidine-HCl. The data marked by asterisks (*) are taken from Maruta and Homma (6).

ferent types of myosins, may act as a signal transducer communicating between the actin-binding site and the ATP binding site along the 25-kDa fragment based on crystallographic studies. The 25-kDa fragment composed mainly of an α-helix, forms the backbone of the myosin head and extends from the actin-binding site to the regulatory region, *via* the ATP binding site, and to the hinge area of the reactive cysteine region. This arrangement means that the 25-kDa fragment and loop M may provide the link through which ATPase activity is modulated by actin.

REFERENCES

1. Rayment, I., Rypniewski, W.R., Schmidt-Base, K., Smith, R., Tomchick, D.R., Benning, M.M., Winkelmann, D.A., Weenberg, G., and Holden, H.M. (1993) Three-dimensional structure of myosin subfragment-1: a molecular motor. *Science* **261**, 50–57
2. Fischer, A.J., Smith, C.A., Thoden, J.B., Smith, R., Sutoh, K., Holden, H.M., and Rayment, I. (1995) X-ray structures of the myosin motor domain of *Dictyostelium discoideum* complexed with MgADP•BeFx and MgADP•AlF_4^-. *Biochemistry* **34**, 8960–8972
3. Dominguez, R., Freyzon, Y., Trybus, K.M., and Cohen, C. (1998) Crystal structure of a vertebrate smooth muscle myosin motor domain and its complex with the essential light chain: visualization of the pre-power stroke state. *Cell* **94**, 559–571
4. Kull, F.J., Sablin, E.P., Lau, R., Fletterick, R.J., and Vale, R.D. (1996) Crystal structure of the kinesin motor domain reveals a structural similarity to myosin. *Nature* **380**, 550–555
5. Maruta, S., Miyanishi, T., and Matsuda, G. (1989) Localization of the ATP-binding site in the 23-kDa and 20-kDa regions of the heavy chain of the skeletal muscle myosin head. *Eur. J. Biochem.* **184**, 213–221
6. Maruta, S. and Homma, K. (1998) A unique loop contributing to the structure of the ATP-binding cleft of skeletal muscle myosin communicates with the actin-binding site. *J. Biochem.* **124**, 528–533
7. Ikebe, M. and Hartshorne, D.J. (1985) Effects of Ca^{2+} on the conformation and enzymatic activity of smooth muscle myosin. *J. Biol. Chem.* **260**, 13146–13153
8. Ikebe, M., Stepinska, M., Kemp, B.E., Means, A.R., and Hartshorne, D.J. (1987) Proteolysis of smooth muscle myosin light chain kinase. Formation of inactive and calmodulin-independent fragments. *J. Biol. Chem.* **262**, 13828–13834
9. Walsh, M.P., Hinkins, S., Dabrowska, R., and Hartshorne, D.J. (1983) Smooth muscle myosin light chain kinase. *Methods Enzymol.* **99**, 279–288
10. Penefsky, H.S. (1977) Reversible binding of P_i by beef heart mitochondrial adenosine triphosphatase. *J. Biol. Chem.* **252**, 2891–2899
11. Luo, Y., Wang, D., Cremo, C.R., Pate, E., Cooke, R., and Yount, R.G. (1995) Photoaffinity ADP analogs as covalently attached reporter groups of the active site of myosin subfragment 1. *Biochemistry* **34**, 1978–1987
12. Laemmli, U.K. (1970) Cleavage of structural proteins during the assembly of the head of bacteriophage T4. *Nature* **227**, 680–685
13. Youngburg, G.E. and Youngburg, M.V. (1930) Phosphorus

metabolism: I. A system of blood phosphorus analysis. *J. Lab. Clin. Med.* **16**, 158–166
14. Maruta, S., Henry, G.D., Sykes, B.D., and Ikebe, M. (1993) Formation of the stable myosin-ADP-aluminum fluoride and myosin-ADP-beryllium fluoride complexes and their analysis using 19F NMR. *J. Biol. Chem.* **268**, 7093–7100
15. Werber, M.M., Peyser, Y.M., and Muhlrad, A. (1992) Characterization of stable beryllium fluoride, aluminum fluoride, and vanadate containing myosin subfragment 1-nucleotide complexes. *Biochemistry* **31**, 7190–7197
16. Phan, B. and Reisler, E. (1992) Inhibition of myosin ATPase by beryllium fluoride. *Biochemistry* **31**, 4787–4793
17. Homma, K. and Maruta, S. (1999) Conformational change of the unique loops in the entrance of the ATP binding site of myosin along the ATPase cycle. *Biophys. J.* **76**, 50a
18. Henry, G.D., Maruta, S., Ikebe, M., and Sykes, B.D. (1993) Observation of multiple myosin subfragment 1-ADP-fluoroberyllate complexes by ^{19}F NMR spectroscopy. *Biochemistry* **32**, 10451–10456
19. Maruta, S., Henry, G.D., Ohki, T., Kambara, T., Sykes, B.D., and Ikebe, M. (1998) Analysis of stress in the active site of myosin accompanied by conformational changes in transient state intermediate complexes using photoaffinity labeling and ^{19}F-NMR spectroscopy. *Eur. J. Biochem.* **252**, 520–529
20. Smith, C.A. and Rayment, I. (1996) X-ray structure of the magnesium(II)•ADP•vanadate complex of the *Dictyostelium discoideum* myosin motor domain to 1.9 Å resolution. *Biochemistry* **35**, 5404–5417